



Cite this: *Dalton Trans.*, 2024, **53**, 4922

Received 19th January 2024,
Accepted 13th February 2024

DOI: 10.1039/d4dt00172a

rsc.li/dalton

Metal–metal cooperativity boosts Lewis basicity and reduction properties of the bis(gallanediyl) $\text{CyL}_2\text{Ga}_2^{\ddagger}$

Christoph Helling,^a Lotta Döhler,^c Oleksandr Kysliak,^c Helmar Görls,^c
Phil Liebing,^c Christoph Wölper,^a Robert Kretschmer^b *^{c,d,e} and
Stephan Schulz^b *^{a,b}

The interplay of two proximate gallium centres equips the bimetallic complex CyL_2Ga_2 (**1**, $\text{CyL}_2 = 1,2\text{-trans-Cy}[\text{NC}(\text{Me})\text{C}(\text{H})\text{C}(\text{Me})\text{N}(\text{Dip})]_2$, Dip = 2,6-*i*-Pr₂C₆H₃) with increased Lewis basicity and higher reducing power compared to the monometallic gallanediyl LGa (**2**, L = HC[MeCN(Dip)]₂) as evidenced by cross-over experiments. Quantum chemical calculations were employed to support the experimental findings.

Introduction

Homobimetallic low-valent main-group metal complexes with metal–metal bonds have attracted increasing attention as their unusual bonding situation and unique frontier molecular orbital arrangements enable transition-metal like reactivity including small molecule activation and catalysis.¹ In addition, molecular complexes with only loosely associated or proximate, yet distinct, low-valent main group centres facilitate chemical transformations unavailable with the corresponding monometallic complexes by bimetallic cooperation.² Unfortunately, metal–metal cooperativity between low-valent main-group metal centres has not yet been studied in full detail due to the scarceness of such compounds. Terphenyl-

substituted group 13 diyls [MAR] (M = Al, Ga, In, Tl) often form weakly associated dimetallenes in the solid-state, whereas they typically dissociate into the corresponding monomeric species in solution.³ Power and co-workers demonstrated experimentally and computationally that the reactions of [2,6-Dip₂C₆H₃]Ga (Dip = 2,6-*i*-Pr₂C₆H₃) towards H₂ and ethylene is mediated *via* the Ga–Ga bonded digallene [(2,6-Dip₂C₆H₃)Ga]₂, whereas monomeric [2,6-Trip₂-3,5-*i*-Pr₂C₆H₃]Ga (Trip = 2,4,6-*i*-Pr₃C₆H₂) was found to be unreactive.⁴

Recently, Kretschmer and co-workers reported bis(metallanediyl) complexes X[NC(Me)C(H)C(Me)N(Dip)M]₂ (X = linker group, M = Ga, In, Tl), in which two monovalent group 13 metal centres are embedded in a single bis(β-diketiminato) ligand framework.⁵ Remarkably, the dinuclear Ga^I complex, CyL_2Ga_2 (**1**, $\text{CyL}_2 = 1,2\text{-trans-Cy}[\text{NC}(\text{Me})\text{C}(\text{H})\text{C}(\text{Me})\text{N}(\text{Dip})]_2$), exhibits enhanced reactivity in the C–F bond activation of fluoroarenes compared to its monometallic counterpart LGa (**2**, L = HC[C(Me)N(Dip)]₂).^{5d} Furthermore, **1** enables the construction of unusual intermetallic compounds for example with group 13 and 15 compounds.^{5e} Computations revealed that a second isomer of **1**, in which the two ambiphilic Ga^I centres interact by forming an intramolecular donor–acceptor complex (**1'**, Fig. S30[†]), is only slightly higher in energy and should hence be accessible at room temperature.^{5d} The isomer **1'** should feature an increased Lewis basicity compared to **2** as one gallium centre donates electron density to the second and hence increases its donor capabilities. Furthermore, the formation of a Ga–Ga bond upon the oxidative addition should equip **1** with increased reducing power compared to the mononuclear species. Herein, we report the results of cross-over experiments between **1** and donor–acceptor complexes as well as halogenated compounds $\text{CyL}_2\text{Ga}_2\text{X}_2$ (**1-X**₂; X = Cl **1-Cl**₂, I **1-I**₂), undoubtedly proving the enhanced reactivity of **1** compared to **2**.

Results and discussion

To prove our hypothesis on the increased Lewis basicity of **1** compared to **2**, we first synthesised the Lewis acid–base

^aInstitute of Inorganic Chemistry, University of Duisburg-Essen, 45117 Essen, Germany. E-mail: stephan.schulz@uni-due.de

^bCenter for Nanointegration Duisburg-Essen (CENIDE), University of Duisburg-Essen, 45117 Essen, Germany

^cInstitute of Inorganic and Analytical Chemistry (IAAC), Friedrich Schiller University Jena, 07743 Jena, Germany. E-mail: robert.kretschmer@chemie.tu-chemnitz.de

^dJena Center for Soft Matter (JCSM), Friedrich Schiller University Jena, 07743 Jena, Germany

^eInstitute of Chemistry, Chemnitz University of Technology, 09111 Chemnitz, Germany

†The work is dedicated to Dietmar Stalke on the occasion of his 65th birthday.

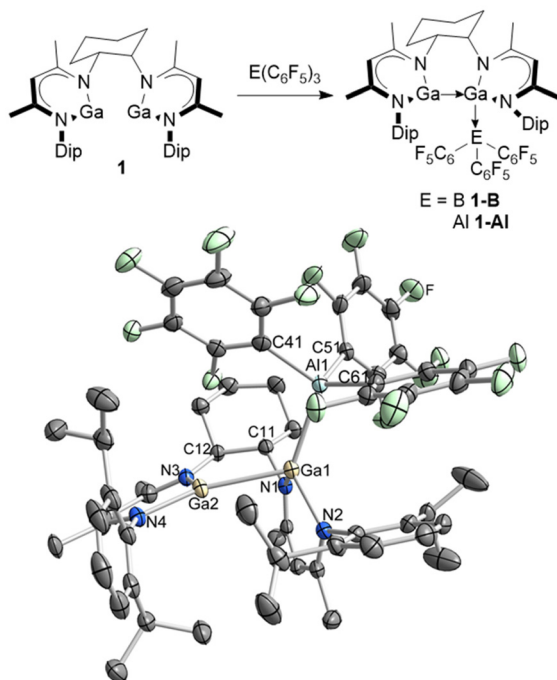
‡Electronic supplementary information (ESI) available: Spectroscopic (NMR and IR), crystallographic and computational data. CCDC 2128586 (**2**-(TEMPO)₂), 2128587 (**1-Al**), 2128588 (**1-Cl**₂), 2128594 (**S1**), 2129461 (**1-I**₂) and 2132253 (**1**-(TEMPO)₄). For ESI and crystallographic data in CIF or other electronic format see DOI: <https://doi.org/10.1039/d4dt00172a>

§Current address: School of Chemistry, Monash University, PO Box 23, Melbourne, VIC, 3800, Australia.



adducts **1-E**(C₆F₅)₃ (E = B **1-B**, Al **1-AI**) by reaction of **1** with equimolar amounts of E(C₆F₅)₃ (Scheme 1, top). Based on *in situ* ¹H, ¹¹B and ¹⁹F NMR spectra, **1-B** forms quantitatively in solution but could not be isolated due to its fast decomposition during work-up. However, the nature of compound **1-B** is established by use of multinuclear (¹H, ¹³C, ¹¹B, ¹⁹F) NMR spectroscopy. In contrast, **1-AI** forms selectively within 12 h at ambient temperature and was obtained after work-up as a yellow crystalline solid in moderate yield (44%).

1-AI is stable in the solid-state under inert gas atmosphere but slowly decomposes in solution to yet unidentified products. The ¹H and ¹³C{¹H} NMR spectra of **1-B** and **1-AI** reflect the asymmetry of the molecules due to the adduct formation, resulting in two distinct sets of resonances for the inequivalent β-diketimate moieties. The ¹¹B NMR resonance of **1-B** (−18.7 ppm) is in a comparable region as observed for **2-B**(C₆F₅)₃ (−20.3 ppm) and Cp*Ga–B(C₆F₅)₃ (−17.9^{6a}/−19.6 ppm;⁷ Cp* = C₅Me₅), hence allowing no conclusions on the donor capability of **1**. The ¹⁹F NMR spectrum of **1-AI** shows the expected three signal pattern, indicating three equivalent C₆F₅ groups, whereas **1-B** features a more complex spectrum containing distinct signals for each fluorine nucleus, potentially due to additional secondary Ga...F interactions⁸ or restricted Ga–B bond rotation. Single crystals of **1-AI** were obtained from a saturated benzene solution by storage at room temperature (Scheme 1, bottom). Its molecular solid-state structure confirms the formation of a rare Ga^I–Al^{III} Lewis acid–base adduct,



Scheme 1 (Top) Synthesis of **1-B** and **1-AI**. (Bottom) Molecular structure of **1-AI** in the solid-state. Hydrogen atoms, the minor component of the disordered *i*-Pr group, and co-crystallised benzene molecules were omitted for clarity. Displacement ellipsoids are drawn at 50% probability level.

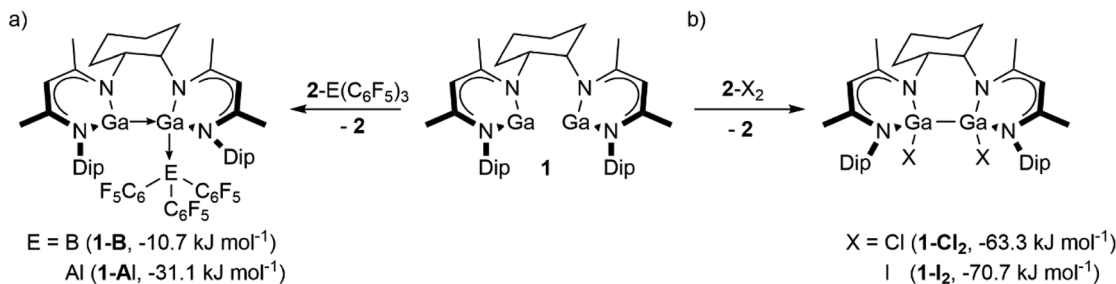
of which only three examples have yet been structurally characterised.^{6b,9} The almost planar six-membered C₃N₂Ga ring containing Ga2 coordinates to Ga1 of the nearly perpendicularly oriented second gallacycle, which additionally coordinates to Al1 of the Al(C₆F₅)₃ moiety, hence creating a virtually planar coordination environment at Ga2 (sum of bond angles: 358.9(3)°) and distorted tetrahedral coordination geometries at Ga1 and Al1, respectively. The Ga1–Ga2 (2.6109(6) Å) bond is longer than the electron-sharing bonds of ^{Cy}L₂Ga(F)Ga(Ar^F) (2.4196(5)–2.4520(8) Å)^{5d} and the dative interactions in **2-Ga**(C₆F₅)₃ (2.4819(2) Å)^{6b} and Cp*Ga–GaX₂Cp* (X = Cl 2.4245(3) Å, I 2.437(2) Å),⁷ respectively, but resembles the computed Ga–Ga bond length of **1'** (2.67 Å).^{5d} The Ga1–Al1 (2.5494(13) Å) bond length is identical to that of **2-Al**(C₆F₅)₃ (2.5482(4) Å),^{6b} consistent with dative Ga2→Ga1 (Ga^I Ga^I) and Ga1 Al1 (Ga^I Al^{III}) bonding interactions. The sum of the C–Al–C bond angles in **1-AI** (323.4(5)°) is smaller than those in Cp*Ga–Al(C₆F₅)₃ (344.6 (1)°, 338.3(1)°^{9a} and **2-Al**(C₆F₅)₃ (334.1(2)°),^{6b} suggesting a stronger Ga–Al interaction in accordance with an increased donor strength of **1**.¹⁰

Next, we conducted cross-over experiments between the known LGa–E(C₆F₅)₃ adducts (**2-E**(C₆F₅)₃; E = B **2-B**, Al **2-AI**)⁶ and ^{Cy}L₂Ga₂ **1** (Scheme 2a), which were monitored by ¹H NMR spectroscopy (Fig. S19 and S20[†]). Addition of **1** to solutions of **2-E**(C₆F₅)₃ immediately afforded bright yellow solutions of **1-B** and **1-AI**, respectively, and compound **2** (Scheme 2a). Despite the relatively small energy gain (*vide infra*), a variable-temperature (VT) ¹H NMR study on the reaction mixture of **1/2-B** (Fig. S23[†]) showed no indication of a temperature-dependent equilibrium, while the addition of an excess of **2** (Fig. S24[†]) did not result in the formation of **2-B**(C₆F₅)₃ and liberation of **1**, thus supporting an irreversible Lewis acid transfer. The cross-over experiments proved the enhanced Lewis basicity of **1** compared to **2**, which is likely induced by the Ga^I–Ga^I donor–acceptor interaction. Similar cross-over experiments of ^{Cy}L₂Ga₂ **1** with LAl–B(C₆F₅)₃ (**3-B**, L = HC[MeCN(Dip)]₂, Fig. S25[†]) showed no conversion even at elevated temperatures, proving the stronger Lewis basic character of LAl (**3**) compared to **1**. However, the significance of the experiment might be biased due to additional Al–F interaction in **3-B**.⁸

Quantum chemical calculations at the BP86(D3-BJ)/def2-SVP level of theory¹¹ were conducted to gain mechanistic insights and the computational findings support the experimental results. The cross-over reactions of the **1/2-E**(C₆F₅)₃ couples are both exergonic, but the gain in energy is more pronounced for the reaction of ^{Cy}L₂Ga₂ **1** with **2-AI** (−31.1 kJ mol^{−1}) as compared to the reaction with **2-B** (−10.7 kJ mol^{−1}). For the **1/2-B**(C₆F₅)₃ couple, we could locate an S_N2-type transition structure on the potential-energy surface associated with a small barrier of only 13.3 kJ mol^{−1}, Fig. S28[†] which agrees well with the observed smooth reaction progress. In contrast, the reaction of **1** with **3-B** is endergonic by 52.1 kJ mol^{−1}, in line with its non-occurrence in our experiments.

Since low-valent group 13 β-diketimate complexes can act as two-electron reductants,¹² we studied the reducing capability of **1** by probing the reductive dehalogenation of LGaX₂





Scheme 2 Cross-over experiments for the evaluation of (a) the Lewis basicity and (b) the reduction capabilities of **1** compared to its mononuclear relative **2** along with the calculated Gibbs free energies at the BP86(D3-BJ)/def2-SVP level of theory.

($2-X_2$; $X = Cl, I$) with **1**, Scheme 2b. In order to identify the expected reaction products, *i.e.*, ${}^{Cy}L_2Ga_2X_2$ (**1-X₂**; $X = Cl$ **1-Cl₂**, **1-I₂**), these were independently synthesised by reactions of **2** with $InCl_3$ (**1-Cl₂**, 29%) and AuI (**1-I₂**, 56%), respectively (Scheme S1†). Compounds **1-Cl₂** and **1-I₂** are stable in the solid-state and in solution under air- and moisture-free conditions. The 1H and ${}^{13}C\{^1H\}$ NMR spectra of **1-Cl₂** and **1-I₂** each exhibit two distinct sets of resonances for the two β -diketiminato moieties despite the nominally symmetric nature of the molecules, arising from a fixed conformation of the *trans*-cyclohexylene-bridge caused by the strain in the polycyclic ring system.

Single-crystals of **1-Cl₂** and **1-I₂** were obtained from saturated solutions in *n*-hexane at ambient temperature and toluene at $5^\circ C$, respectively (Fig. S23 and S25†). The halide substituents in the dihalogallanes adopt *syn*-periplanar conformations with respect to the Ga–Ga bond (torsion angles X–Ga–Ga–X: **1-Cl₂** $13.92(2)^\circ$, **1-I₂** $1.64(3)^\circ$), which contrasts with non-bridged dihalogallanes containing β -diketiminato¹³ and diazabutadienide¹⁴ ligands that adopt *syn*-clinal and *anti*-periplanar conformations, respectively. The Ga–Ga and Ga–X bond lengths in **1-Cl₂** (Ga–Ga 2.4185(3) Å; Ga–Cl 2.2159(4) Å, 2.2327(3) Å) and **1-I₂** (Ga–Ga 2.4615(6) Å; Ga–I 2.6337(6) Å, 2.5779(6) Å) are comparable to those of related dihalogallanes (Ga–Ga 2.242–2.576 Å; Ga–Cl 2.210–2.218 Å; Ga–I 2.586–2.633 Å)^{13,14} based on non-bridging ligands and those of ${}^{Cy}L_2Ga(F)Ga(Ar^F)$ (2.4196(5)–2.4520(8) Å),^{5d} indicating covalent Ga^{II}–Ga^{II} and Ga^{II}–X bonding interactions.

The cross-over experiments between $2-X_2$ and **1** were then monitored by 1H NMR spectroscopy (Scheme 2b and Fig. S21, S22†). While no reaction occurred at ambient temperature, heating the reaction mixtures to $90^\circ C$ for 2 days (**1-Cl₂**) and $70^\circ C$ for 5 days (**1-I₂**) resulted in the irreversible consumption of **1** and $2-X_2$ as well as liberation of **2** and formation of **1-Cl₂** and **1-I₂**, respectively, which were identified by 1H NMR spectroscopy (Fig. S21 and S22†). **1-Cl₂** and **1-I₂** are formed together with small amounts of yet unidentified side products, altering the reaction stoichiometry. This likely results from the higher reaction temperatures required to overcome the activation barrier for the halogen transfer imposed by the sterically demanding environments of the Ga centres in **1** and **2**. However, the cross-over experiments undoubtedly proved the

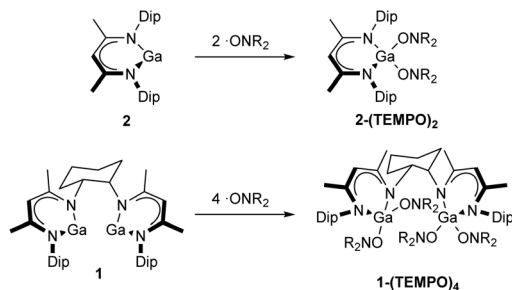
higher reducing power of binuclear **1** compared to mononuclear **2**. The reactions are consistent with one-electron oxidation per Ga centre each in **1** and a two-electron reduction of the Ga centre in $2-X_2$, while the *syn*-periplanar arrangement of the halide substituents in **1-Cl₂** and **1-I₂** supports a suprafacial addition of the halogen atoms to **1**.

In contrast, **1** failed to react with LaI_2 (**3-I₂**) even at elevated temperatures (Fig. S26†), indicating a stronger reduction potential of LaI (**3**) compared to **1**. This reaction may be additionally hampered by the larger steric congestion of the Al centre due to the slightly shorter Al–N and Al–I bond lengths, respectively.¹⁵ These findings agree with the computations according to which the dehalogenation of $2-X_2$ is exergonic by 63.3 ($X = Cl$) and 70.7 kJ mol^{-1} ($X = I$) but endergonic by 53.0 kJ mol^{-1} in case of **3-I₂**. We also tried to compute the reaction pathway but despite repeated attempts, we could not locate the respective transition structures. However, we could identify two local minima *en route* $1 + 2-X_2 \rightarrow 1-X_2 + 2$, Fig. S29,† these are a formal encounter complex of **1** and $2-X_2$ and an intermediate in which one halogen each is bound to **1** and **2**, respectively.

Aiming to identify a general preference of compound **1** to form the corresponding Ga^{II}–Ga^{II} complexes instead of two separate Ga^{III} moieties, we investigated the reactions of compounds **1** and **2** with the aminoxyl radical TEMPO (2,2,6,6-tetramethylpiperidine-*N*-oxyl, $\cdot ONR_2$). Gallanediyl **2** cleanly reacts with two equivalents of TEMPO with oxidation of the Ga^I centre (Scheme 3) and formation of $LGa(TEMPO)_2$ ($2-(TEMPO)_2$), which was isolated as pale yellow crystals in high yield (78%).

$2-(TEMPO)_2$ features the expected resonances in its 1H and ${}^{13}C\{^1H\}$ NMR spectra, and its molecular constitution was confirmed by sc-XRD (Fig. S26†). Similarly, bis(gallanediyl) **1** reacts with four equivalents of TEMPO to give ${}^{Cy}L_2Ga_2(TEMPO)_4$ (**1-(TEMPO)₄**) containing two discrete Ga^{III} centres (Scheme 3) in 29% yield; using a 1:2 stoichiometry provided a mixture of **1** and **1-(TEMPO)₄**. **1-(TEMPO)₄** was characterised by sc-XRD (Fig. S27†), whereas no meaningful NMR spectra could be obtained due to its poor solubility in common organic solvents. The Ga centres in $2-(TEMPO)_2$ and **1-(TEMPO)₄** are distorted tetrahedrally coordinated and feature Ga–O bond lengths ($2-(TEMPO)_2$ 1.8505(19) Å, 1.8555(15) Å; **1-**





Scheme 3 Synthesis of 2-(TEMPO)₂ and 1-(TEMPO)₄ (NR₂ = N(Me₂CCH₂)₂CH₂).

(TEMPO)₄ 1.833(6) Å, 1.850(7) Å) in the expected range. These results show that all four electrons of the two Ga^I centres in 1 are in principle available for oxidation reactions.

Experimental

General procedures

All manipulations were carried out under an atmosphere of purified argon using standard Schlenk and glovebox techniques. Toluene and *n*-hexane were dried with an MBraun Solvent Purification System, and benzene was distilled from Na/K alloy. Deuterated benzene was dried over activated molecular sieves (4 Å) and degassed prior to use. Starting materials ^{Cy}L₂Ga₂ (1),^{5d} LGa (2),¹⁶ B(C₆F₅)₃,¹⁷ Al(C₆F₅)₃(toluene),¹⁸ LGa-B(C₆F₅)₃ (2-B(C₆F₅)₃),^{6a} LGa-Al(C₆F₅)₃ (2-Al(C₆F₅)₃),^{6b} LGaCl₂ (2-Cl₂),¹⁵ and LGaI₂ (2-I₂)¹⁵ were prepared according to literature procedures. AuI, InCl₃, and TEMPO were obtained from commercial sources and used as received. NMR spectra (δ in ppm) were recorded using a Bruker Avance DPX 300 (¹H 300.1 MHz, ¹³C{¹H} 75.5 MHz, ¹¹B 96.3 MHz, ¹⁹F 282.4 MHz), a Bruker Avance Neo 400 (¹H 400.1 MHz, ¹³C{¹H} 100.6 MHz, ¹¹B 128.4 MHz, ¹⁹F 376.5 MHz), or a Bruker Avance III HD (¹H 600.1 MHz, ¹³C{¹H} 150.9 MHz, ¹¹B 192.5 MHz, ¹⁹F 564.7 MHz) spectrometer and were referenced to internal C₆D₅H (¹H δ = 7.16, ¹³C δ = 128.06), external BF₃(OEt₂) (¹¹B δ = 0.00), or external CFCl₃ (¹⁹F δ = 0.00) standards. IR spectra were recorded in a glovebox either with an Agilent Cary 630 FTIR or an ALPHA-T FT-IR spectrometer both equipped with a single-reflection ATR sampling module. Microanalyses were performed at the elemental analysis laboratory of the University of Duisburg-Essen. Melting points were measured in wax-sealed glass capillaries under argon atmosphere using a Thermo Scientific 9300 apparatus and are uncorrected.

Synthetic procedures

Synthesis of ^{Cy}L₂Ga₂-B(C₆F₅)₃ (1-B). ^{Cy}L₂Ga₂ (10 mg, 0.0136 mmol) and B(C₆F₅)₃ (7 mg, 0.0136 mmol) were dissolved in C₆D₆ (0.5 mL) resulting in a bright yellow solution, which was subjected to NMR spectroscopic analysis, indicating the clean formation of 1-B. Several attempts to isolate 1-B as a pure material failed due to facile decomposition. ¹H NMR

(400.1 MHz, C₆D₆): δ 7.25 (br d, ³J_{HH} = 7.8 Hz, 1 H, C₆H₃(i-Pr)₂), 7.20 (t, ³J_{HH} = 7.7 Hz, 1 H, C₆H₃(i-Pr)₂), 7.04 (m, 2 H, C₆H₃(i-Pr)₂), 7.00 (dd, *J*_{HH} = 7.5, 1.5 Hz, 1 H, C₆H₃(i-Pr)₂), 6.88 (dd, *J*_{HH} = 6.6, 2.5 Hz, 1 H, C₆H₃(i-Pr)₂), 4.91 (s, 1 H, γ-CH), 4.56 (s, 1 H, γ-CH), 3.79 (dt, *J*_{HH} = 10.9, 3.5 Hz, 1 H, NCH), 3.70 (m, 1 H, NCH), 2.86 (m, 2 H, CH(CH₃)₂), 2.43 (m, 2 H, CH(CH₃)₂), 1.74 (s, 3 H, CCH₃), 1.60 (s, 3 H, CCH₃), 1.55 (m, 1 H, CH₂), 1.49 (m, 1 H, CH₂), 1.39 (s, 3 H, CCH₃), 1.32 (m, 2 H, CH₂), 1.28 (d, ³J_{HH} = 6.8 Hz, 3 H, CH(CH₃)₂), 1.18 (m, 1 H, CH₂), 1.11 (s, 3 H, CCH₃), 1.04 (d, ³J_{HH} = 6.7 Hz, 3 H, CH(CH₃)₂), 1.01 (d, ³J_{HH} = 6.7 Hz, 3 H, CH(CH₃)₂), 0.97 (d, ³J_{HH} = 6.7 Hz, 3 H, CH(CH₃)₂), 0.94 (d, ³J_{HH} = 6.8 Hz, 3 H, CH(CH₃)₂), 0.89 (d, ³J_{HH} = 6.7 Hz, 3 H, CH(CH₃)₂), 0.85 (d, ³J_{HH} = 6.7 Hz, 3 H, CH(CH₃)₂), 0.80 (d, ³J_{HH} = 6.8 Hz, 3 H, CH(CH₃)₂), 0.67 (m, 3 H, CH₂). ¹³C NMR (100.6 MHz, C₆D₆): δ 168.3 (CCH₃), 168.0 (CCH₃), 167.1 (CCH₃), 165.8 (CCH₃), 147.8 (C₆H₃(i-Pr)₂), 145.1 (C₆H₃(i-Pr)₂), 144.3 (C₆H₃(i-Pr)₂), 143.1 (C₆H₃(i-Pr)₂), 142.2 (C₆H₃(i-Pr)₂), 139.2 (C₆H₃(i-Pr)₂), 127.1 (C₆H₃(i-Pr)₂), 125.4 (C₆H₃(i-Pr)₂), 125.1 (C₆H₃(i-Pr)₂), 124.3 (C₆H₃(i-Pr)₂), 124.2 (C₆H₃(i-Pr)₂), 104.3 (γ-CH), 104.2 (γ-CH), 64.1 (NCH), 62.7(NCH), 38.6 (CH₂), 30.5 (CH₂), 30.1 (CH(CH₃)₂), 29.8 (CH(CH₃)₂), 28.8 (CH(CH₃)₂), 28.5 (CH(CH₃)₂), 26.0 (CH(CH₃)₂), 25.8 (CH₂ & CH(CH₃)₂), 25.4 (CH₂ & CH(CH₃)₂), 25.2 (CCH₃), 25.2 (CH(CH₃)₂), 24.6 (CH₂), 24.1 (CH(CH₃)₂), 23.5 (CCH₃), 23.2 (CH(CH₃)₂), 23.2 (CH(CH₃)₂), 22.8 (CCH₃), 22.7 (CH(CH₃)₂), 21.9 (CCH₃) (C₆F₅ not observed). ¹¹B NMR (128.4 MHz, C₆D₆): δ -18.7 (s, 1 B, B(C₆F₅)₃). ¹⁹F NMR (376.5 MHz, C₆D₆): δ -120.9 (br s, 1 F, *o*-C₆F₅), -122.3 (br s, 1 F, *o*-C₆F₅), -122.6 (br s, 1 F, *o*-C₆F₅), -129.0 (br s, 1 F, *o*-C₆F₅), -129.8 (br s, 1 F, *o*-C₆F₅), -133.7 (br s, 1 F, *o*-C₆F₅), -160.9 (t, ³J_{FF} = 20.7 Hz, 1 F, *p*-C₆F₅), -162.6 (t, ³J_{FF} = 19.6 Hz, 1 F, *p*-C₆F₅), -163.5 (br s, 1 F, *p*-C₆F₅), -164.1 (br s, 2 F, *m*-C₆F₅), -164.3 (br s, 2 F, *m*-C₆F₅), -165.1 (br s, 1 F, *m*-C₆F₅), -167.5 (br s, 1 F, *m*-C₆F₅).

Synthesis of ^{Cy}L₂Ga₂-Al(C₆F₅)₃ (1-Al). ^{Cy}L₂Ga₂ (50 mg, 0.0681 mmol) and Al(C₆F₅)₃(tol) (42 mg, 0.0681 mmol) were dissolved in toluene (2 mL) and the resulting yellow solution was stirred for 24 h at ambient temperature. The solution was slightly concentrated and stored at -30 °C overnight to afford yellow analytically pure crystals of 1-Al. Single-crystals suitable for X-ray diffraction were obtained from a saturated benzene solution at ambient temperature. Yield: 38 mg (0.0301 mmol, 44%). Mp: 196 °C (dec.). Anal. calcd for C₅₈H₅₈AlF₁₅Ga₂N₄: C, 55.18; H, 4.63; N, 4.44. Found: C, 55.5; H, 5.00; N, 4.47. ¹H NMR (400.1 MHz, C₆D₆): δ 7.07 (m, 3 H, C₆H₃(i-Pr)₂), 6.97 (d, ³J_{HH} = 7.6 Hz, 1 H, C₆H₃(i-Pr)₂), 6.83 (m, 2 H, C₆H₃(i-Pr)₂), 4.93 (s, 1 H, γ-CH), 4.66 (s, 1 H, γ-CH), 3.92 (t, ³J_{HH} = 10.4 Hz, 1 H, NCH), 3.47 (t, ³J_{HH} = 9.9 Hz, 1 H, NCH), 3.20 (sept, ³J_{HH} = 6.7 Hz, 1 H, CH(CH₃)₂), 3.14 (sept, ³J_{HH} = 6.7 Hz, 1 H, CH(CH₃)₂), 2.57 (sept, ³J_{HH} = 6.7 Hz, 1 H, CH(CH₃)₂), 2.29 (d, ³J_{HH} = 12.5 Hz, 1 H, CH₂), 2.20 (sept, ³J_{HH} = 6.7 Hz, 1 H, CH(CH₃)₂), 1.63 (s, 3 H, CCH₃), 1.51 (m, 1 H, CH₂), 1.46 (s, 3 H, CCH₃), 1.39 (s, 3 H, CCH₃), 1.36 (s, 3 H, CCH₃), 1.34 (m, 2 H, CH₂), 1.19 (m, 1 H, CH₂), 1.15 (d, ³J_{HH} = 6.7 Hz, 3 H, CH(CH₃)₂), 1.10 (d, ³J_{HH} = 6.7 Hz, 3 H, CH(CH₃)₂), 1.05 (d, ³J_{HH} = 6.8 Hz, 3 H, CH(CH₃)₂), 1.02 (d, ³J_{HH} = 6.8 Hz, 3 H, CH(CH₃)₂), 0.99 (d, ³J_{HH} = 6.8 Hz,



3 H, CH(CH₃)₂), 0.95 (d, ³J_{HH} = 6.7 Hz, 3 H, CH(CH₃)₂), 0.86 (m, 1 H, CH₂), 0.78 (m, 1 H, CH₂), 0.73 (d, ³J_{HH} = 6.7 Hz, 3 H, CH(CH₃)₂), 0.61 (m, 1 H, CH₂), 0.23 (d, ³J_{HH} = 6. Hz, 3 H, CH(CH₃)₂). ¹³C NMR (100.6 MHz, C₆D₆): δ 171.5 (CCH₃), 169.2 (CCH₃), 168.9 (CCH₃), 165.8 (CCH₃), 151.3 (C₆F₅), 149.0 (C₆F₅), 143.8 (C₆H₃(i-Pr)₂), 143.7 (C₆H₃(i-Pr)₂), 143.3 (C₆H₃(i-Pr)₂), 142.7 (C₆H₃(i-Pr)₂), 141.6 (C₆H₃(i-Pr)₂), 141.2 (C₆H₃(i-Pr)₂), 138.3 (C₆F₅), 135.9 (C₆F₅), 125.3 (C₆H₃(i-Pr)₂), 124.6 (C₆H₃(i-Pr)₂), 124.4 (C₆H₃(i-Pr)₂), 124.1 (C₆H₃(i-Pr)₂), 103.2 (γ-CH), 99.3 (γ-CH), 66.4 (NCH), 66.4 (NCH), 37.7 (CH₂), 33.0 (CH₂), 29.6 (CH(CH₃)₂), 28.6 (CH(CH₃)₂), 28.3 (CH(CH₃)₂), 25.9 (CH₂), 25.8 (CH(CH₃)₂), 25.6 (CH₂), 25.2 (CH(CH₃)₂), 24.6 (CH(CH₃)₂), 24.5 (CH(CH₃)₂), 24.4 (CCH₃), 24.3 (CH(CH₃)₂), 23.9 (CCH₃), 23.9 (CCH₃), 23.8 (CCH₃), 23.6 (CH(CH₃)₂), 23.4 (CH(CH₃)₂), 22.9 (CH(CH₃)₂). ¹⁹F NMR (376.5 MHz, C₆D₆): δ -118.1 (br s, 6 F, *o*-C₆F₅), -156.4 (t, ³J_{FF} = 19.8 Hz, 3 F, *p*-C₆F₅), -162.6 (m, 3 F, *m*-C₆F₅). IR (neat): ν 2950, 2917, 2861, 1632, 1537, 1501, 1430, 1370, 1314, 1257, 1051, 1015, 950, 794, 759, 681, 604, 494, 430 cm⁻¹.

Synthesis of ^{Cy}L₂Ga₂Cl₂ (1-Cl₂). InCl₃ (15 mg, 0.0681 mmol) was added to a solution of ^{Cy}L₂Ga₂ (50 mg, 0.0681 mmol) in benzene (1 mL) and the resulting suspension was stirred for 4 h. The reaction mixture was filtered, and volatiles were removed from the filtrate *in vacuo*. The residue was washed with *n*-hexane (3 × 2.5 mL) and dried under reduced pressure affording **1-Cl₂** as a pale yellow solid. Single-crystals suitable for X-ray diffraction were obtained from a saturated solution in *n*-hexane at ambient temperature. Yield: 16 mg (0.0199 mmol, 29%). Mp: 266 °C (dec.). Anal. calcd for C₄₀H₅₈Cl₂Ga₂N₄: C, 59.66; H, 7.26; N, 6.96. Found: C, 59.8; H, 7.09; N, 6.71. ¹H NMR (400.1 MHz, C₆D₆): δ 7.21 (dd, *J*_{HH} = 7.7, 1.8 Hz, 1 H, C₆H₃(i-Pr)₂), 7.17 (t, ³J_{HH} = 7.5 Hz, 1 H, C₆H₃(i-Pr)₂), 7.11 (m, 3 H, C₆H₃(i-Pr)₂), 6.94 (m, 1H, C₆H₃(i-Pr)₂), 4.99 (dt, *J*_{HH} = 11.6, 3.7 Hz, 1 H, NCH), 4.57 (s, 1 H, γ-CH), 4.56 (s, 1 H, γ-CH), 3.93 (sept, ³J_{HH} = 6.6 Hz, 1 H, CH(CH₃)₂), 3.60 (dt, *J*_{HH} = 10.9, 5.0 Hz, 1 H, NCH), 3.24 (sept, ³J_{HH} = 6.7 Hz, 1 H, CH(CH₃)₂), 3.16 (sept, ³J_{HH} = 6.7 Hz, 1 H, CH(CH₃)₂), 2.76 (sept, ³J_{HH} = 6.8 Hz, 1 H, CH(CH₃)₂), 2.37 (m, 1 H, CH₂), 2.07 (m, 1 H, CH₂), 1.73 (s, 3 H, CCH₃), 1.63 (m, 2 H, CH₂), 1.60 (s, 3 H, CCH₃), 1.60 (d, ³J_{HH} = 6.7 Hz, 3 H, CH(CH₃)₂), 1.57 (s, 3 H, CCH₃), 1.55 (s, 3 H, CCH₃), 1.52 (d, ³J_{HH} = 6.6 Hz, 3 H, CH(CH₃)₂), 1.45 (m, 1 H, CH₂), 1.40 (m, 2 H, CH₂), 1.25 (d, ³J_{HH} = 6.7 Hz, 3 H, CH(CH₃)₂), 1.19 (d, ³J_{HH} = 6.8 Hz, 3 H, CH(CH₃)₂), 1.06 (d, ³J_{HH} = 6.7 Hz, 3 H, CH(CH₃)₂), 0.96 (d, ³J_{HH} = 6.8 Hz, 3 H, CH(CH₃)₂), 0.85 (m, 1 H, CH₂), 0.77 (d, ³J_{HH} = 6.8 Hz, 3 H, CH(CH₃)₂). ¹³C NMR (100.6 MHz, C₆D₆): δ 167.6 (CCH₃), 167.1 (CCH₃), 166.4 (CCH₃), 165.8 (CCH₃), 147.3 (C₆H₃(i-Pr)₂), 145.1 (C₆H₃(i-Pr)₂), 144.1 (C₆H₃(i-Pr)₂), 142.7 (C₆H₃(i-Pr)₂), 142.2 (C₆H₃(i-Pr)₂), 139.9 (C₆H₃(i-Pr)₂), 127.3 (C₆H₃(i-Pr)₂), 127.3 (C₆H₃(i-Pr)₂), 125.7 (C₆H₃(i-Pr)₂), 124.7 (C₆H₃(i-Pr)₂), 124.3 (C₆H₃(i-Pr)₂), 124.2 (C₆H₃(i-Pr)₂), 98.8 (γ-CH), 97.1 (γ-CH), 62.4 (NCH), 62.2 (NCH), 32.9 (CH₂), 32.5 (CH₂), 30.0 (CH(CH₃)₂), 28.7 (CH(CH₃)₂), 28.4 (CH(CH₃)₂), 27.9 (CH(CH₃)₂), 26.8 (CH(CH₃)₂), 25.7 (CH₂), 25.5 (CH(CH₃)₂), 25.3 (CH₂ & CH(CH₃)₂), 25.0 (CH(CH₃)₂), 25.0 (CH(CH₃)₂), 24.7 (CH(CH₃)₂), 24.6 (CCH₃), 24.5 (CCH₃), 24.3 (CH(CH₃)₂), 21.8 (CCH₃). IR (neat): ν 2951, 2916,

2857, 1556, 1504, 1431, 1375, 1314, 1258, 1188, 1078, 1023, 942, 793, 759, 741, 633, 537, 438 cm⁻¹. N.B.: In.

Synthesis of ^{Cy}L₂Ga₂I₂ (1-I₂). ^{Cy}L₂Ga₂ (98 mg, 0.1300 mmol) and AuI (42 mg, 0.1300 mmol) were suspended in 5 ml of toluene and stirred overnight at room temperature. The solids were filtered off and the volume of the brown/orange filtrate was reduced in vacuum to about 1 ml. Upon storage at 5 °C, yellow crystals of **1-I₂** appeared, which we filtered off, washed with 2.5 ml of toluene and dried in vacuum. Yield: 36 mg (0.0364 mmol, 56%). Mp: 240 °C (dec.). Anal. calcd For C₄₀H₅₈Ga₂N₄I₂: despite repeated attempts, no satisfactory microanalysis could be obtained, most likely due to incomplete removal of co-crystallised solvent. ¹H NMR (400.1 MHz, toluene-d₈): δ 7.15 (m, 2 H, C₆H₃(i-Pr)₂), 7.06 (m, 3 H, C₆H₃(i-Pr)₂), 6.92 (dd, *J*_{HH} = 5.6, 3.5 Hz, 1 H, C₆H₃(i-Pr)₂), 5.03 (br s, 1 H, NCH), 4.59 (s, 1 H, γ-CH), 4.56 (s, 1 H, γ-CH), 3.93 (br s, 1 H, CH(CH₃)₂), 3.74 (dt, *J*_{HH} = 11.0, 5.0 Hz, 1 H, NCH), 3.13 (br s, 2 H, CH(CH₃)₂), 2.63 (m, 2 H, CH(CH₃)₂ & CH₂), 2.19 (br s, 1 H, CH₂), 1.71 (s, 3 H, CCH₃), 1.64 (m, 5 H, CH(CH₃)₂ & CH₂), 1.63 (s, 3 H, CCH₃), 1.62 (s, 3 H, CCH₃), 1.60 (d, ³J_{HH} = 6.6 Hz, 3 H, CH(CH₃)₂), 1.50 (d, ³J_{HH} = 6.7 Hz, 3 H, CH(CH₃)₂), 1.49 (s, 3 H, CCH₃), 1.22 (d, ³J_{HH} = 6.6 Hz, 3 H, CH(CH₃)₂), 1.20 (m, 2 H, CH₂), 1.16 (d, ³J_{HH} = 6.8 Hz, 3 H, CH(CH₃)₂), 1.01 (d, ³J_{HH} = 6.6 Hz, 3 H, CH(CH₃)₂), 0.93 (m, 2 H, CH₂), 0.85 (d, ³J_{HH} = 6.8 Hz, 3 H, CH(CH₃)₂), 0.78 (br d, ³J_{HH} = 5.9 Hz, 3 H, CH(CH₃)₂). ¹³C NMR (100.6 MHz, toluene-d₈): δ 167.4 (CCH₃), 167.2 (CCH₃), 144.6 (C₆H₃(i-Pr)₂), 142.4 (C₆H₃(i-Pr)₂), 127. (C₆H₃(i-Pr)₂), 127.3 (C₆H₃(i-Pr)₂), 124.3 (C₆H₃(i-Pr)₂), 124.2 (C₆H₃(i-Pr)₂), 99.4 (γ-CH), 97.9 (γ-CH), 32.7 (CH₂), 30.3 (CH(CH₃)₂), 28.8 (CH(CH₃)₂), 28.4 (CH(CH₃)₂), 27.8 (CH(CH₃)₂), 25.4 (CH₂), 25.4 (CH(CH₃)₂), 25.3 (CH₂ & CH(CH₃)₂), 24.9 (CH(CH₃)₂), 24.7 (CH(CH₃)₂), 24.3 (CH(CH₃)₂), 22.0 (CCH₃). IR (neat): ν 2958, 2925, 2864, 1556, 1506, 1433, 1377, 1312, 1260, 1189, 1018, 864, 794, 759, 732 cm⁻¹.

Synthesis of ^{Cy}L₂Ga₂(TEMPO)₄ (1-(TEMPO)₄). Toluene (6 mL) was added to a mixture of ^{Cy}L₂Ga₂ (100 mg, 0.14 mmol) and TEMPO (85 mg, 0.545 mmol) at room temperature. Colorless crystals of **1-(TEMPO)₄** formed within 5 minutes and the flask was stored at -30 °C for 3 h. The crystals were separated by filtration and dried in vacuum. Yield: 54 mg (0.040 mmol, 29%). Mp: 187 °C. Anal. calcd for C₇₆H₁₃₀Ga₂N₈O₄: C, 67.15; H, 9.64; N, 8.24. Found: C, 67.51; H, 9.49; N, 7.84. NMR studies were not possible due to the low solubility of **7** in common organic solvents. IR (neat): ν = 2963, 2930, 2870, 1539, 1470, 1396, 1368, 1323, 1267, 1182, 1131, 1044, 1014, 954, 915, 788, 751, 665 cm⁻¹.

Synthesis of LGa(TEMPO)₂ (2-(TEMPO)₂). Benzene (2 mL) was added to a mixture of LGa (50 mg, 0.1026 mmol) and TEMPO (32 mg, 0.2052 mmol) at ambient temperature and the resulting pale yellow solution was stirred for 30 minutes. The solution was concentrated until incipient crystallisation and stored at ambient temperature overnight affording pale yellow analytically pure crystals of **2-(TEMPO)₂**. Yield: 64 mg (0.0800 mmol, 78%). Mp: 249 °C. Anal. calcd for C₄₇H₇₇GaO₂N₄: C, 70.58; H, 9.70; N, 7.00. Found: C, 71.8; H, 10.1; N, 7.00. ¹H NMR (400.1 MHz, C₆D₆): δ 7.21 (m, 6 H,



$C_6H_3(i\text{-Pr})_2$, 4.85 (s, 1 H, $\gamma\text{-CH}$), 4.69 (sept, $^3J_{\text{HH}} = 6.7$ Hz, 1 H, $\text{CH}(\text{CH}_3)_2$), 4.29 (sept, $^3J_{\text{HH}} = 6.7$ Hz, 1 H, $\text{CH}(\text{CH}_3)_2$), 3.45 (sept, $^3J_{\text{HH}} = 6.7$ Hz, 1 H, $\text{CH}(\text{CH}_3)_2$), 3.33 (sept, $^3J_{\text{HH}} = 6.7$ Hz, 1 H, $\text{CH}(\text{CH}_3)_2$), 1.85 (m, 1 H, $\text{CH}_2\text{CH}_2\text{CH}_2$), 1.81 (s, 3 H, $\text{C}(\text{CH}_3)_2$), 1.74 (m, 2 H, $\text{CH}_2\text{CH}_2\text{CH}_2$ & $\text{CH}_2\text{CH}_2\text{CH}_2$), 1.62 (m, 1 H, $\text{CH}_2\text{CH}_2\text{CH}_2$), 1.59 (d, $^3J_{\text{HH}} = 6.7$ Hz, 3 H, $\text{CH}(\text{CH}_3)_2$), 1.55 (d, $^3J_{\text{HH}} = 6.7$ Hz, 3 H, $\text{CH}(\text{CH}_3)_2$), 1.53 (m, 2 H, $\text{CH}_2\text{CH}_2\text{CH}_2$), 1.53 (d, $^3J_{\text{HH}} = 6.7$ Hz, 3 H, $\text{CH}(\text{CH}_3)_2$), 1.52 (d, $^3J_{\text{HH}} = 6.7$ Hz, 3 H, $\text{CH}(\text{CH}_3)_2$), 1.50 (s, 3 H, $\text{C}(\text{CH}_3)_2$), 1.48 (s, 3 H, $\text{C}(\text{CH}_3)_2$), 1.45 (s, 3 H, $\text{C}(\text{CH}_3)_2$), 1.42 (s, 3 H, $\text{C}(\text{CH}_3)_2$), 1.38 (s, 3 H, $\text{C}(\text{CH}_3)_2$), 1.36 (m, 3 H, $\text{CH}_2\text{CH}_2\text{CH}_2$ & $\text{CH}_2\text{CH}_2\text{CH}_2$), 1.28 (d, $^3J_{\text{HH}} = 6.7$ Hz, 3 H, $\text{CH}(\text{CH}_3)_2$), 1.24 (m, 1 H, $\text{CH}_2\text{CH}_2\text{CH}_2$), 1.20 (m, 1 H, $\text{CH}_2\text{CH}_2\text{CH}_2$), 1.15 (d, $^3J_{\text{HH}} = 6.7$ Hz, 3 H, $\text{CH}(\text{CH}_3)_2$), 1.10 (m, 1 H, $\text{CH}_2\text{CH}_2\text{CH}_2$), 1.06 (d, $^3J_{\text{HH}} = 6.7$ Hz, 3 H, $\text{CH}(\text{CH}_3)_2$), 1.01 (s, 3 H, $\text{C}(\text{CH}_3)_2$), 0.96 (s, 3 H, $\text{C}(\text{CH}_3)_2$), 0.72 (s, 3 H, $\text{C}(\text{CH}_3)_2$), 0.42 (s, 3 H, $\text{C}(\text{CH}_3)_2$). $^{13}\text{C}\{\text{H}\}$ NMR (100.6 MHz, C_6D_6): δ 171.1 (CCH_3), 171.0 (CCH_3), 146.1 ($\text{C}_6\text{H}_3(i\text{-Pr})_2$), 145.5 ($\text{C}_6\text{H}_3(i\text{-Pr})_2$), 145.4 ($\text{C}_6\text{H}_3(i\text{-Pr})_2$), 144.4 ($\text{C}_6\text{H}_3(i\text{-Pr})_2$), 143.8 ($\text{C}_6\text{H}_3(i\text{-Pr})_2$), 143.4 ($\text{C}_6\text{H}_3(i\text{-Pr})_2$), 128.6 ($\text{C}_6\text{H}_3(i\text{-Pr})_2$), 127.4 ($\text{C}_6\text{H}_3(i\text{-Pr})_2$), 125.0 ($\text{C}_6\text{H}_3(i\text{-Pr})_2$), 124.9 ($\text{C}_6\text{H}_3(i\text{-Pr})_2$), 124.9 ($\text{C}_6\text{H}_3(i\text{-Pr})_2$), 124.3 ($\text{C}_6\text{H}_3(i\text{-Pr})_2$), 100.0 ($\gamma\text{-CH}$), 61.1 ($\text{C}(\text{CH}_3)_2$), 60.4 ($\text{C}(\text{CH}_3)_2$), 59.3 ($\text{C}(\text{CH}_3)_2$), 59.2 ($\text{C}(\text{CH}_3)_2$), 41.9 ($\text{CH}_2\text{CH}_2\text{CH}_2$), 41.4 ($\text{CH}_2\text{CH}_2\text{CH}_2$), 41.2 ($\text{CH}_2\text{CH}_2\text{CH}_2$), 41.1 ($\text{CH}_2\text{CH}_2\text{CH}_2$), 34.1 ($\text{C}(\text{CH}_3)_2$), 33.8 ($\text{C}(\text{CH}_3)_2$), 33.2 ($\text{C}(\text{CH}_3)_2$), 31.4 ($\text{C}(\text{CH}_3)_2$), 29.0 ($\text{CH}(\text{CH}_3)_2$), 28.8 ($\text{CH}(\text{CH}_3)_2$), 27.7 ($\text{CH}(\text{CH}_3)_2$), 27.2 ($\text{CH}(\text{CH}_3)_2$), 26.3 ($\text{CH}(\text{CH}_3)_2$), 26.2 (CCH_3), 26.0 ($\text{CH}(\text{CH}_3)_2$), 25.9 ($\text{CH}(\text{CH}_3)_2$), 25.7 ($\text{CH}(\text{CH}_3)_2$), 25.5 ($\text{CH}(\text{CH}_3)_2$), 25.4 (CCH_3), 25.0 ($\text{CH}(\text{CH}_3)_2$), 24.7 ($\text{CH}(\text{CH}_3)_2$), 24.2 ($\text{CH}(\text{CH}_3)_2$), 20.8 ($\text{C}(\text{CH}_3)_2$), 20.6 ($\text{C}(\text{CH}_3)_2$), 20.4 ($\text{C}(\text{CH}_3)_2$), 20.1 ($\text{C}(\text{CH}_3)_2$), 18.1 ($\text{CH}_2\text{CH}_2\text{CH}_2$), 18.0 ($\text{CH}_2\text{CH}_2\text{CH}_2$). IR (neat): $\nu = 2966, 2929, 2869, 1523, 1437, 1398, 1319, 1254, 1179, 1018, 937, 862, 787, 761, 678, 523, 447$ cm^{-1} .

Computations

All geometry optimisations and frequency calculations were performed with the Gaussian16 program package¹⁹ in conjunction with the BP86 functional^{11a,b} and def2-SVP basis sets.^{11c} The D3 version of Grimme's dispersion correction with the Becke–Johnson damping function was applied to account for dispersion effects.^{11d} The absence of imaginary frequencies confirmed stationary points as minima. All energies (given in kJ mol^{-1}) are corrected by the (unscaled) zero-point vibrational energy and by thermal energies at 298.15 K.

Crystallography

The crystals of **1-Al**, **2-Cl**₂, **2-I**₂, **1-(TEMPO)**₄, **2-(TEMPO)**₂, and **S1** were mounted on nylon loops in inert oil. Crystallographic data of **1-Al**, **1-Cl**₂, **2-(TEMPO)**₂, and **S1** were collected on a Bruker D8 Kappa diffractometer with APEX2 detector (Mo- K_α radiation, $\lambda = 0.71073$ Å) at 100(2) K. Absorption corrections were performed semi-empirically from equivalent reflections on the basis of multiscans (Bruker AXS APEX2). The intensity data of **2-I**₂ and **1-(TEMPO)**₄ were collected on a Nonius KappaCCD diffractometer using graphite-monochromated Mo- K_α radiation. Data were corrected for Lorentz and polarisation effects; absorption was taken into account on a semi-empirical

basis using multiple-scans.²⁰ The crystallographic data are summarised in Tables S1 and S2.† The structures were solved by direct methods (SHELXS-97²¹ and SHELXS²²) and refined anisotropically by full-matrix least-squares on F^2 (SHELXL-2017 and SHELXL-2018).²³ Hydrogen atoms were refined using a riding model or rigid methyl groups. In **1-Al**, an *i*-Pr group is disordered over two positions. Its bond lengths and angles were restrained to be equal (SADI) and RIGU restraints were applied to its atoms' displacement parameters. Due to their close proximity, C35 and C35' were refined with common displacement parameters (EADP). A benzene molecule is strongly disordered over a centre of inversion. Two alternate positions could be identified of which one is on the centre of inversion. The local symmetry of these positions was ignored in the refinement (negative PART). The bond lengths and angles of all solvent molecules were restrained to be equal (SADI) and the atoms were restrained to lie on a common plane (FLAT). RIGU restraints were applied to the anisotropic displacement parameters. Additionally, for residue 3 ISOR restraints were used. In **1-Cl**₂, the cyclohexylene ring is disordered over two positions. The displacement of the smaller component could only be refined isotropically and EADP constraints had to be applied to displacement parameters of C11 and C11' to avoid correlations with the occupancy. In addition, one chlorine atom is disordered over two positions. The Cl–Ga bond lengths of both components were restrained to be equal (SADI). One of the *i*-Pr groups (C10–C12) of **1-I**₂ is disordered. The disorder could be resolved to a ratio of 65:35%. The crystal of **1-(TEMPO)**₄ was treated as a twin by 180° rotation and additionally by inversion. Determination of the twinned cell was performed with CellNow, whereas TWINABS was used for data reduction and absorption correction.²⁴ The two *i*-Pr groups of **1-(TEMPO)**₄ are disordered. The disorder could be resolved to ratios of 69:31% (C15–C17) and 54:46% (C18–C20), respectively. On the crystal of **2-(TEMPO)**₂ there was a small satellite crystal that could not be removed. Treatment as non-merohedral twin revealed its reflections to be very weak ($I < 1\sigma$). Including the second component had no influence on the model thus the twinning/satellite could be ignored. The absolute structure of **S1** could be determined reliably. Parsons' quotient method was used to determine the absolute structure parameter x .²⁵

Conclusions

To conclude, the superior basicity and enhanced reducing capability of bimetallic **1** compared to its monometallic counterpart **2** were unambiguously demonstrated by cross-over experiments involving Lewis acid and halogen transfer reactions. The increased reactivity of **1** is attributed to an interaction between the Ga^I centres. Such synergistic interactions in low-valent bimetallic complexes are expected to play a crucial role in main group element-mediated bond activation processes and catalytic transformations in the future.



Author contributions

C. H. conceived the fundamental scheme of the study, executed the experimental work with support by L. D. and O. K., while R. K. performed the quantum chemical calculations. C. W., H. G., and P. L. conducted the sc-XRD measurements and processed the corresponding data. R. K. and S. S. supervised the study. The manuscript was written by C. H., R. K., and S. S.

Conflicts of interest

There are no conflicts to declare.

Acknowledgements

Financial support by the Deutsche Forschungsgemeinschaft (SCHU 1069/23-1, INST 20876/282-1 FUGG, KR4782/3-1, KR4782/2-4), the Chemnitz University of Technology (R. K.), and the Open Access Publication Fund of the University of Duisburg-Essen (S. S.) is acknowledged. We are thankful to S. H. Schreiner for analytic support (IR, melting points) and to the Rechenzentrum of the Friedrich Schiller University Jena for the allocation of computer time.

References

- (a) T. Chu and G. I. Nikonov, *Chem. Rev.*, 2018, **118**, 3608; (b) P. P. Power, *Nature*, 2010, **463**, 171; (c) C. Weetman and S. Inoue, *ChemCatChem*, 2018, **10**, 4213; (d) S. Yadav, S. Saha and S. S. Sen, *ChemCatChem*, 2015, **8**, 486; (e) P. P. Power, *Chem. Rev.*, 1999, **99**, 3463; (f) R. C. Fischer and P. P. Power, *Chem. Rev.*, 2010, **110**, 3877; (g) P. P. Power, *Organometallics*, 2020, **39**, 4127; (h) F. Hanusch, L. Groll and S. Inoue, *Chem. Sci.*, 2021, **12**, 2001; (i) H. B. Wedler, P. Wendelboe and P. P. Power, *Organometallics*, 2018, **37**, 2929; (j) C. Shan, S. Yao and M. Driess, *Chem. Soc. Rev.*, 2020, **49**, 6733.
- (a) J. Campos, *Nat. Rev. Chem.*, 2020, **4**, 696; (b) J. M. Gil-Negrete and E. Hevia, *Chem. Sci.*, 2021, **12**, 1982; (c) N. Villegas-Escobar, A. Toro-Labbé and H. F. Schaefer III, *Chem. – Eur. J.*, 2021, **27**, 17369.
- (a) J. D. Queen, A. Lehmann, J. C. Fettingler, H. M. Tuononen and P. P. Power, *J. Am. Chem. Soc.*, 2020, **142**, 20554; (b) N. J. Hardman, R. J. Wright, A. D. Phillips and P. P. Power, *Angew. Chem., Int. Ed.*, 2002, **41**, 2842; (c) N. J. Hardman, R. J. Wright, A. D. Phillips and P. P. Power, *J. Am. Chem. Soc.*, 2003, **125**, 2667; (d) Z. Zhu, R. C. Fischer, B. D. Ellis, E. Rivard, W. A. Merrill, M. M. Olmstead, P. P. Power, J. D. Guo, S. Nagase and L. Pu, *Chem. – Eur. J.*, 2009, **15**, 5263; (e) S. T. Haubrich and P. P. Power, *J. Am. Chem. Soc.*, 1998, **120**, 2202; (f) R. J. Wright, A. D. Phillips, N. J. Hardman and P. P. Power, *J. Am. Chem. Soc.*, 2002, **124**, 8538; (g) M. Niemeyer and P. P. Power, *Angew. Chem., Int. Ed.*, 1998, **37**, 1277; (h) R. J. Wright, A. D. Phillips, S. Hino and P. P. Power, *J. Am. Chem. Soc.*, 2005, **127**, 4794.
- C. A. Caputo, J. Koivistoinen, J. Moilanen, J. N. Boynton, H. M. Tuononen and P. P. Power, *J. Am. Chem. Soc.*, 2013, **135**, 1952.
- (a) M. E. Desat, S. Gärtner and R. Kretschmer, *Chem. Commun.*, 2017, **53**, 1510; (b) M. E. Desat and R. Kretschmer, *Chem. – Eur. J.*, 2018, **24**, 12397; (c) M. E. Desat and R. Kretschmer, *Dalton Trans.*, 2019, **48**, 17718; (d) O. Kysliak, H. Görls and R. Kretschmer, *J. Am. Chem. Soc.*, 2021, **143**, 142; (e) C. Helling, J. C. Farmer, C. Wölper, R. Kretschmer and S. Schulz, *Organometallics*, 2023, **42**, 72.
- (a) N. J. Hardman, P. P. Power, J. D. Gordon, C. L. B. Macdonald and A. H. Cowley, *Chem. Commun.*, 2001, 1866; (b) C. Ganesamoorthy, M. Matthias, D. Bläser, C. Wölper and S. Schulz, *Dalton Trans.*, 2016, **45**, 11437.
- P. Jutzi, B. Neumann, G. Reumann, L. O. Schebaum and H.-G. Stammer, *Organometallics*, 2001, **20**, 2854.
- Z. Yang, X. Ma, R. B. Oswald, H. W. Roesky, H. Zhu, C. Schulzke, K. Starke, M. Baldus, H.-G. Schmidt and M. Noltemeyer, *Angew. Chem., Int. Ed.*, 2005, **44**, 7072.
- (a) J. D. Gordon, C. L. B. MacDonald and A. H. Cowley, *Main Group Chem.*, 2005, **4**, 33; (b) S. Schulz, A. Kuczkowski, D. Schuchmann, U. Flörke and M. Nieger, *Organometallics*, 2006, **25**, 5487.
- (a) H. Jacobsen, H. Berke, S. Döring, G. Kehr, G. Erker, R. Fröhlich and O. Meyer, *Organometallics*, 1999, **18**, 1724; (b) A. H. Cowley, *Chem. Commun.*, 2004, 2369.
- (a) A. D. Becke, *Phys. Rev. A*, 1998, **38**, 3098; (b) J. P. Perdew, *Phys. Rev. B: Condens. Matter Mater. Phys.*, 1986, **33**, 8822; (c) F. Weigend and R. Ahlrichs, *Phys. Chem. Chem. Phys.*, 2005, **7**, 3297; (d) S. Grimme, S. Ehrlich and L. Goerigk, *J. Comput. Chem.*, 2011, **32**, 1456; (e) B. Metz, H. Stoll and M. Dolg, *J. Chem. Phys.*, 2000, **113**, 2563; (f) K. A. Peterson, D. Figgen, E. Goll, H. Stoll and M. Dolg, *J. Chem. Phys.*, 2003, **119**, 11113.
- M. Zhong, S. Sinhababu and H. W. Roesky, *Dalton Trans.*, 2020, **49**, 1351.
- R. Laubenstein, M. Ahrens and T. Braun, *Z. Anorg. Allg. Chem.*, 2017, **643**, 1723.
- (a) R. J. Baker, R. D. Farley, C. Jones, D. P. Mills, M. Kloth and D. M. Murphy, *Chem. – Eur. J.*, 2005, **11**, 2972; (b) Y. Zhao, Y. Liu, Q.-S. Li and J.-H. Su, *Dalton Trans.*, 2016, **45**, 246.
- M. Stender, B. E. Eichler, N. J. Hardman, P. P. Power, J. Prust, M. Noltemeyer and H. W. Roesky, *Inorg. Chem.*, 2001, **40**, 2794.
- N. J. Hardman, B. E. Eichler and P. P. Power, *Chem. Commun.*, 2000, 1991.
- A. G. Massey and A. J. Park, *J. Organomet. Chem.*, 1964, **2**, 245.
- G. S. Hair, A. H. Cowley, R. A. Jones, B. G. McBurnett and A. Voigt, *J. Am. Chem. Soc.*, 1999, **121**, 4922.



- 19 M. J. Frisch, G. W. Trucks, H. B. Schlegel, G. E. Scuseria, M. A. Robb, J. R. Cheeseman, G. Scalmani, V. Barone, G. A. Petersson, H. Nakatsuji, X. Li, M. Caricato, A. V. Marenich, J. Bloino, B. G. Janesko, R. Gomperts, B. Mennucci, H. P. Hratchian, J. V. Ortiz, A. F. Izmaylov, J. L. Sonnenberg, D. Williams-Young, F. Ding, F. Lipparini, F. Egidi, J. Goings, B. Peng, A. Petrone, T. Henderson, D. Ranasinghe, V. G. Zakrzewski, J. Gao, N. Rega, G. Zheng, W. Liang, M. Hada, M. Ehara, K. Toyota, R. Fukuda, J. Hasegawa, M. Ishida, T. Nakajima, Y. Honda, O. Kitao, H. Nakai, T. Vreven, K. Throssell, J. A. Montgomery Jr, J. E. Peralta, F. Ogliaro, M. J. Bearpark, J. J. Heyd, E. N. Brothers, K. N. Kudin, V. N. Staroverov, T. A. Keith, R. Kobayashi, J. Normand, K. Raghavachari, A. P. Rendell, J. C. Burant, S. S. Iyengar, J. Tomasi, M. Cossi, J. M. Millam, M. Klene, C. Adamo, R. Cammi, J. W. Ochterski, R. L. Martin, K. Morokuma, O. Farkas, J. B. Foresman and D. J. Fox, *Gaussian 16, Revision C.01*, Gaussian, Inc., Wallingford CT, 2016.
- 20 (a) *COLLECT*, *Data Collection Software*, Nonius B.V., Netherlands, 1998; (b) Z. Otwinowski and W. Minor, Processing of X-Ray Diffraction Data Collected in Oscillation Mode, in *Methods in Enzymology*, ed. C. W. Carter and R. M. Sweet, *Macromolecular Crystallography, Part A*, Academic Press, 1997, vol. 276, pp. 307–326; (c) SADABS 2016/2: L. Krause, R. Herbst-Irmer, G. M. Sheldrick and D. Stalke, *J. Appl. Crystallogr.*, 2015, **48**, 3.
- 21 G. M. Sheldrick, *Acta Crystallogr., Sect. A: Found. Crystallogr.*, 1990, **46**, 467–473.
- 22 G. M. Sheldrick, *Acta Crystallogr., Sect. A: Found. Adv.*, 2015, **71**, 3–8.
- 23 (a) G. M. Sheldrick, *SHELXL-2014, Program for the Refinement of Crystal Structures*; University of Göttingen, Göttingen, Germany, 2014. See also: G. M. Sheldrick, *Acta Crystallogr., Sect. A: Found. Crystallogr.*, 2008, **64**, 112; (b) shelXle, A Qt GUI for SHELXL: C. B. Hübschle, G. M. Sheldrick and B. Dittrich, *J. Appl. Crystallogr.*, 2011, **44**, 1281; (c) G. M. Sheldrick, *Acta Crystallogr., Sect. C: Struct. Chem.*, 2015, **71**, 3.
- 24 Bruker, *Apex III, CellNow and TWINABS*, Bruker AXS Inc., Madison, Wisconsin, USA, 2012.
- 25 (a) S. Parsons and H. D. Flack, *Acta Crystallogr., Sect. A: Found. Crystallogr.*, 2004, **60**, s61; (b) S. Parsons, H. D. Flack and T. Wagner, *Acta Crystallogr., Sect. B: Struct. Sci., Cryst. Eng. Mater.*, 2013, **69**, 249.

